PHYSICAL REVIEW B VOLUME 31, NUMBER 11 1 JUNE 1985

Pressure dependence of intramolecular and intermolecular mode frequencies in solid oxygen determined by Raman studies

H. J. Jodl,* F. Bolduan, and H. D. Hochheimer
Max-Planck-Institut für Festkörperforschung, Heisenbergstrasse 1, D-7000 Stuttgart 80, Federal Republic of Germany

(Received 18 June 1984)

Solid molecular oxygen was investigated in a diamond anvil cell by Raman spectroscopy in the region of 6—300 K with pressures up to 14 GPa. Characteristic spectral features in the different crystalline phases of oxygen allow conclusions to be drawn about the p-T phase diagram. The splitting of the vibrational Raman line in γ-O_2 is explained by a vibration-vibration resonant transfer between molecules on different sites in the lattice. In addition, the effect of pressure on intermolecular and intramolecular forces, which causes a pressure dependence of mode-Grüneisen parameters, is investigated. Finally, anharmonic contributions to the potential are calculated from independent measurements of $(\partial \nu/\partial p)_T$ and $(d\nu/dT)_p$, allowing the separation of the anharmonicities into pure volume and multiphonon contributions.

I. INTRODUCTION

Solid molecular oxygen combines properties of both a molecular crystal and of a magnetic material. The magnetic moment of O_2 arises from the two unpaired outer-shell electrons ($S=1$) in the electronic ground state $^3\Sigma_g^-$ and is directed perpendicular to the molecular axis. Therefore, in addition to the weak intermolecular and strong intramolecular forces characteristic for molecular crystals, magnetic interactions will play an important role. In particular they account for special crystalline configurations, depending on the ordering of the magnetic moments.

Thus solid oxygen shows an antiferromagnetic order in the low-temperature α phase which is stable up to 23.7 K at zero pressure.[1] Its structure is monoclinic with space group $C2/m$ (C_{2h}^3) and one molecule per primitive cell.[2,3] All molecules are colinear and perpendicular to the basal (a,b) plane.

At atmospheric pressure the rhombohedral β phase with space group $R\bar{3}m$ (D_{3d}^5) and one molecule per primitive cell is stable between 23.7 and 43.8 K.[4,5] All molecules are colinear and perpendicular to the hexagonal basal plane. Only short-range antiferromagnetic order is present with a three-sublattice structure arranged in such a way that all nearest-neighbor magnetic moments are oriented at 120° with respect to each other.[3]

The cubic γ phase with space group $Pm3n$ (Ref. 6) existing from 43.8 K to the melting point at 54.4 K (Ref. 1) shows an orientationally disordered structure with eight molecules in the primitive cell. There are two molecules on $m3(T_h)$ sites which are randomly orientated about the crystal C_3 symmetry axis and six molecules on $\bar{4}2m$ (D_{2d}) sites which take random orientations about the crystal C_2 axis. For more details about these low-temperature configurations see Refs. 7 and 8.

As known from high-pressure x-ray measurements the rhombohedral β phase extends up to room temperature[9] and even up to at least 600 K.[10] At 300 K a new configuration known as α'-O_2 (orange O_2) was identified between 9.5 and 10.0 GPa by single-crystal x-ray diffraction studies.[11] The structure is orthorhombic with space group $Fmmm$ (D_{2h}^{23}) and four molecules per unit cell. Above 10 GPa at 300 K another new high-pressure phase was found,[9] referred to as ϵ-O_2, whose structure could not be determined until now.

Optical investigations (ir, Raman) of several crystalline phases of oxygen were performed. In accordance with group-theoretical predictions vibrational and librational modes can be observed in the Raman spectra. In the antiferromagnetic α phase one A_g vibrational and two-librational modes with A_g and E_g symmetry are Raman active and have already been observed in Raman spectra at zero pressure.[12] In addition two magnon modes at $\sim$6 and $\sim$27 cm^{-1} were investigated either by ir (Refs. 13—15) and/or Raman scattering (Refs. 16 and 17) in this phase.

In the Raman spectrum of the rhombohedral β phase only one librational mode with E_g symmetry shows up in addition to the A_g vibron.[12] The Raman spectrum of γ-O_2 is characterized by a vibrational doublet resulting from molecules on the two nonequivalent sites in the $Pm3n$ lattice.[18—20] The splitting is 1.3 cm^{-1} at zero pressure and the observed intensity ratio is 3:1, in accordance with the occupation ratio of the two sites which is 6:2. The low-energy Raman spectrum, however, reveals, in addition to the Rayleigh wing, a broad structureless hump which is characteristic of a rotationally disordered system.[12]

The high-pressure orthorhombic $Fmmm$ phase has two librational modes with B_{2g} and B_{3g} symmetry, which were observed recently, as well as one A_g vibrational mode.[21] The present knowledge of the p-T phase diagram of oxygen in the low-temperature region is based either on volume investigations[22] or on susceptibility measurements,[23] whereas the region above 200 K in an extended pressure range was mainly studied by optical techniques such as Raman scattering[20,24] or by direct observation of color changes (absorption) of the sample which accom-

©1985 The American Physical Society

pany the β-α and α'-ϵ phase transitions.[10,24] The results of all these investigations are compiled in the p-T phase diagram of oxygen, shown in Fig. 1. In addition to open questions about the connection of phase boundaries between low- and high-pressure regions (thus between low and high temperatures), discrepancies also arise in comparing data of Nicol *et al.*[24] and Yagi *et al.*[10] concerning the liquid-β, β-α', and α'-ϵ phase boundaries.

One aim of our investigations was the determination of phase boundaries and thus the completion of the p-T phase diagram of oxygen. Raman scattering has proven to be useful for this purpose because of its adaptibility to high-pressure diamond anvil technique. As will be shown later the different phases exhibit characteristic spectral features either in the vibrational or librational part. In some cases these features are unique and can be used to identify unambiguously the presence of a special phase. In other cases the spectral features are not unique (e.g., α and α' phase) and one must look for other indications of the occurrence of phase transition, i.e., frequency shifts or discontinuities in the pressure dependence of the vibrational and librational mode frequencies. A second aspect of this work deals with the investigation of the intermolecular and intramolecular potentials and their anharmonic contributions which cause a pressure and temperature dependence of the mode frequencies. A third aim is to compare our experimental results with theory as far as possible concerning the pressure dependence of vibrational and librational modes in α-O_2.[25,26] Finally, an interesting aspect is offered by the peculiar pressure behavior of the intensities of the two vibrational components in γ-O_2. This effect will be explained by resonant V-V transfer coupling between molecules on two different sites in the lattice of γ-O_2.

II. EXPERIMENTAL

The Raman measurements were performed with a high-pressure diamond anvil cell described in Ref. 27. The samples were prepared in the following way. The cell with a small ruby chip inside the sample chamber for pressure calibration[28] was mounted in a cryostat with the movable stem holding the upper diamond fixed above the gasket, providing a spacing between the diamond and the gasket of about 0.3 mm. This spacing is large enough to allow the liquified oxygen to flow below the upper diamond and to fill the sample hole in the Inconel gasket. After the cell was cooled to 80 K, gaseous oxygen (purity 99.999%) was led inside through a thin capillary attached just beside the sample hole in the Inconel gasket. After the gas had liquified, which could be observed from outside by a microscope, the cell was closed and the liquid was pressurized to a few kilobars.

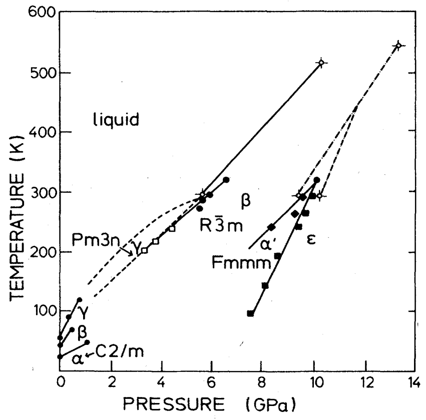

FIG. 1. p-T phase diagram of molecular oxygen prior to our work. The phase boundaries in the low-temperature region are taken from Refs. 22 and 23: ●, □, ■, data from Ref. 24; ○, Ref. 10; the dashed line is taken from Ref. 20.

Temperature was measured either by a Pt-100 or a germanium resistor with an accuracy of 0.5 K and a stability of 0.2 K for many hours. The sensor was attached directly beside the gasket. As He gas was used as a heat-conducting medium a very continuous heat transfer was possible between the high-pressure cell and the coolant. Therefore temperature gradients, unavoidable in bath cryostates, where cooling is only provided through heat transfer from the cell to the bath mediated by a cooling flange, were negligible in our case.

Special care was taken to avoid local heating during laser irradiation. The precise knowledge of the actual sample temperature was especially necessary for the determination of the p-T phase diagram. With a maximum power of 200 mW (5145 Å) no significant laser heating was observed, as checked carefully by the following experiments.

(1) The temperature shift of the ruby fluorescence line R_1, known from the literature,[28] was measured after focusing the laser spot directly on the ruby chip.

(2) Intensity measurements ($I_{\text{anti}}/I_{\text{Stokes}}$) for the low-frequency Raman spectrum yielded an estimation for the local temperature.

(3) When cooled down at zero pressure, the α-β and β-γ phase-transition temperatures were measured and compared with those from the literature.[1,22]

These three independent checks led to the conclusion that in our case laser heating was less than 3 K.

The Raman equipment consisted of a double-grating monochromator in connection with a third monochromator, a Peltier-cooled photomultiplier tube (C31034), and a standard photon-counting system. The experimental procedure for gathering spectroscopic data was the following: Spectra were always recorded at fixed temperatures (isothermal conditions) with increasing pressure starting from the liquid state to avoid hysteresis effects on crossing phase boundaries. At temperatures below the melting point at zero pressure the pressure was released to zero before each run. All spectra were calibrated with spectral lines of an Ar lamp with an accuracy of 0.3—0.5 cm^{-1} for the vibration and 0.5—2 cm^{-1} for the librations, depending on line intensity and width.

III. RESULTS AND DISCUSSION

A. Description of the spectra

Figure 2 shows a collection of low-energy Raman spectra of solid oxygen in different phases. Three phases can

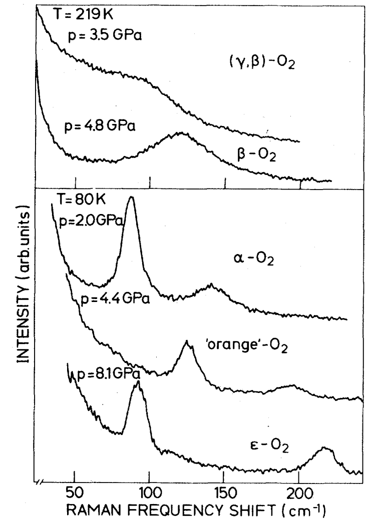

FIG. 2. Raman spectra of solid oxygen in the low-energy region.

easily be recognized by mere observation of the spectra. There is a broad single band (E_g) in β-O_2, an extended Rayleigh wing in γ-O_2, and two modes (A_g,B_g) in α-O_2, as already known from zero-pressure experiments.[12]

The spectrum of α'-O_2 (orange O_2) with two modes B_{2g} and B_{3g} (Ref. 21) is similar to that of α-O_2, which will be discussed later. The ϵ phase shows also two modes but with a different intensity pattern compared to α-O_2.

For various fixed temperatures, pressure runs were done by recording the vibrational and librational Raman frequencies. One example of this is shown in Fig. 3 for the case of 80 K. Some indications of phase transitions are evident in Fig. 3, such as changes in the number of modes, distinct changes in the pressure coefficients $(\partial\nu/\partial p)_T$ (especially for the vibron) or discontinuities in the pressure dependence of special modes, and differences in the intensity patterns of the spectra.

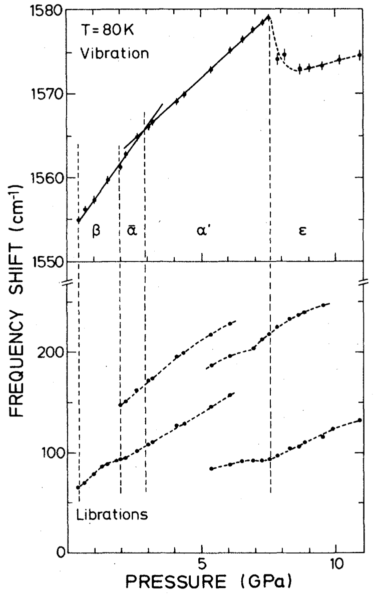

FIG. 3. Pressure dependence of the vibrational and librational energies of solid oxygen at 80 K.

Thus the γ-β and β-α (β-α') phase transitions can be clearly identified by looking at the low-energy Raman spectra. The liquid-γ and γ-β transitions are marked by the appearance and disappearance, respectively, of a doublet in the vibrational Raman line (see Figs. 4 and 7).

The frequency-pressure relation of the vibron can be approximated very well by a straight line in all phases up to 7.5 GPa. However, the slope of this line is slightly different for each phase. Above 7.5 GPa a sudden decrease of frequency of 4—5 cm^{-1} is observed, demonstrated in Fig. 3 for the case of 80 K. This drop in frequency can be observed at all temperatures up to at least 300 K and is interpreted as due to the phase transition to the so-called ϵ configuration.[9,24] This sudden drop is also accompanied by an abrupt change of color of the sample from nearly transparent to dark red. In addition, the two librational Raman lines markedly grow in intensity, in contrast to the range between 5.5 and 7.8 GPa, where these two lines are extremely weak. Most probably the region where these two lines are present in the spectrum, together with the two lines of the α' phase, can be interpreted as a region where α'- and ϵ-O_2 coexist. This behavior can be observed for temperatures up to 120 K. At higher temperatures the four lines of this coexistence region broaden and smear out, especially the lines characteristic of ϵ-O_2, which are merely detectable in the coexistence region.

Other hints for phase transitions follow from the distinct change in the pressure dependence, especially of the vibron near 3 GPa (see Figs. 3 and 5). This distinct change of the pressure coefficient $(\partial\nu/\partial p)_T$ is observed in all pressure runs for temperatures below 105 K. Above this temperature this effect is missing and the pressure coefficient does not change up to the α'-ϵ transition. Only a slight decrease of 0.5 cm^{-1} is measured on crossing the β-α' boundary, an effect which cannot be represented using the scale of Fig. 4. Thus this behavior near 3 GPa for temperatures below 105 K is most probably a hint for a phase transition. A similar and more drastic change of $(\partial\nu/\partial p)_T$ is observed in pressure runs below 30 K at nearly 0.5 GPa, for the vibrons as well as for the librons (Fig. 5). The same effect has been noticed by Meier *et al.*,[29] who report such a change in the slope of the pressure

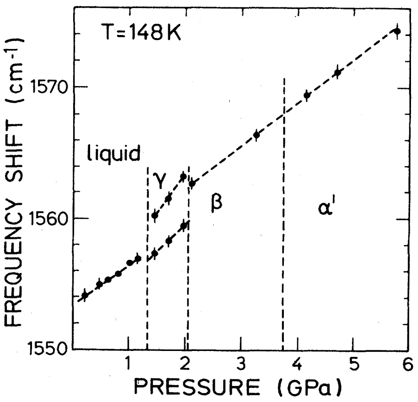

FIG. 4. Pressure dependence of the vibron energy at 148 K.

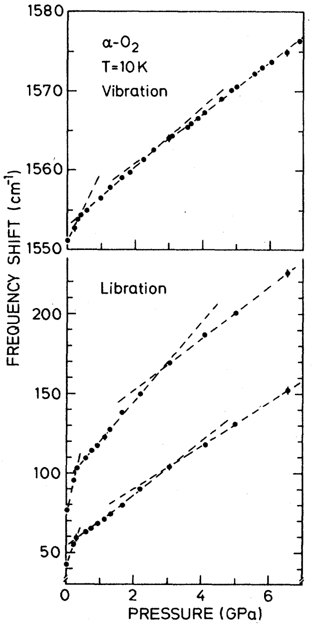

FIG. 5. Pressure-dependent vibron and libron frequencies of solid oxygen at 10 K.

dependence at 0.8—1.1 GPa. The discrepancy with our pressure value of 0.5 GPa is most probably due to inaccurate pressure calibration in their work.

In addition, the kink at 3 GPa, especially for the vibron, was not seen in their work because of too few data points in that region. As a result these two changes at 0.5 and 3 GPa, especially observed for the vibron, can be interpreted to be caused by phase transitions. The fact that in both cases any discontinuities in the Raman frequencies are missing and that the general features of the Raman spectra are the same, leads to the conclusion that the structure of the oxygen lattice does not change drastically during these two transitions. The discussion about this will be continued in the next section.

B. p-T phase diagram of oxygen

The results of the measurements described in Sec. III A can be used to construct a p-T phase diagram which is presented in Fig. 6. For the sake of simplicity this graph contains only our experimentally determined phase boundaries.

For temperatures below 120 K our liquid-γ, γ-β, and β-α boundaries coincide with earlier data.[1,22,23] Concerning the γ-phase boundaries, good agreement can also be seen comparing our work with that of Yen *et al.*[20] Thus the liquid-γ-β triple point is located at 286±4 K and 5.4±0.2 GPa.

Discrepancies are evident between our data and those of d'Amour *et al.*[9] concerning the high-pressure data of the liquid-β, β-α', and α'-ϵ phase boundaries. All their curves are shifted to lower temperatures compared to ours. Indeed, their values were revised in a recent paper by Yagi *et al.*,[10] in which the temperature range was extended up to 600 K. Thus the β-α'-ϵ triple point can be extrapolated to lie near 440 K and 11.5 GPa in accordance with estimations from our data.

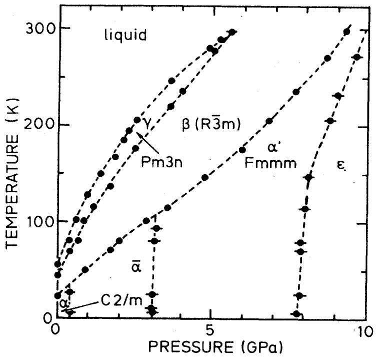

FIG. 6. p-T phase diagram of oxygen determined from our Raman experiments.

Open questions remain in the low-temperature region between 0.5 and 3 GPa. As we interpret the changes in $(\partial\nu/\partial p)_T$ to be due to phase transitions, most probably a new configuration of solid oxygen exists between 0.5 and 3 GPa (denoted $\bar{\alpha}$). Theoretical considerations of Helmy *et al.*[26] predict a phase transition at $T=0$ K and 0.6 GPa without any change in volume from the monoclinic α phase to an orthorhombic phase, which could be similar or even equal to the α' structure, identified at 9.6 GPa at room temperature.[11] Both structures are, indeed, closely related. Only a small change of the monoclinic angle β and perhaps a slight reorientation of the molecules perpendicular to the basal plane transforms the one structure into the other. This transition, driven by a simple shear, should occur with little volume change. The general spectroscopic features as far as the number of lines and their intensities are concerned do not change in our experiment in the pressure range of 0 to 7 GPa below 30 K. Only the pressure shift $(\partial\nu/\partial p)_T$ changes for both the vibron and librons at the values noted above. These observations lead to the conclusion that the unit cell does not change drastically across these two phase transitions.

Our suggestion is that the onset of the α' configuration at low temperatures is near 3 GPa and, thus, between 0.5 and 3 GPa a new low-temperature and high-pressure phase exists (tentatively called $\bar{\alpha}$), the structure of which is closely related to both the α and α' structures. Perhaps this phase is characterized by a different magnetic ordering compared to the antiferromagnetic α structure. Unfortunately the magnetic susceptibility measurements of Meier *et al.*[23] were only performed up to 0.5 GPa and therefore cannot give hints about the magnetic structure above 0.5 GPa or even about the occurrence of a phase transition to support our assumption.

In this sense the pressure dependence of the magnon modes, observed at ~6 and ~27 cm^{-1} at zero pressure,[16,17] would be of great help for the solution of this problem. Unfortunately these modes could not be seen in our spectra because of too-low intensity due to the small sample dimension (70 μm thickness). As known from earlier Raman investigations,[16,17] the intensity of the 27 cm^{-1} magnon line is about 1% of the intensity of the lowest-energy libration in α-O$_2$. Furthermore the 6 cm^{-1} line would not have been resolvable from the intense Rayleigh light with our Raman equipment.

At the end of this section the peculiar behavior of the vibron in ϵ-O_2 will be discussed. After the sudden drop in energy, there is a smooth decrease and, after passing a broad minimum, the pressure dependence is almost linear with a shift of 3 cm^{-1}/GPa, which extends to 40 GPa at room temperature.[30] It was concluded from this and additional measurements in that region[31] that the molecular axes are probably not parallel and compression between the α'-ϵ transition point (sudden drop of the vibron frequency) and the onset of the linear frequency-pressure relationship causes a reorientation of molecular axes. However, until a structure analysis has been done, no definite explanation can be given for this behavior.

C. Splitting of the vibron in γ-O_2

As described in the Introduction, the vibrational Raman line splits into a doublet in γ-O_2 at zero pressure. This splitting is caused by the molecules occupying two nonequivalent sites in this phase. The intensity ratio of both components reflects the occupation ratio of these two sites, known to be 6:2 in the unit cell.

In our experiment at higher pressures this doublet shows an increase of the splitting with increasing pressure and a continuous change of the intensity ratio of both components (Fig. 7). At zero pressure the ratio is 3:1 for the lower-frequency component and the splitting is 1.3 cm^{-1} (Ref. 19) and increases to 5 cm^{-1} at 5 GPa (Fig. 7).

At 3 GPa and 200 K both components have equal intensities and for even higher pressures the intensity of the higher-frequency component exceeds that of the lower one. This peculiar intensity behavior with pressure can be explained by a coupling of the vibrational motions of molecules of different sites, the so-called V-V resonant transfer coupling. The description is similar to the case of the "Fermi-resonance interaction" for degenerate vibrational levels with equal symmetry in polyatomic molecules. Therefore the same formalism can be used for the description of the V-V coupling in γ-O_2. Guissani *et al.*[32] have developed a suitable formalism applying perturbation theory. As a result the interaction can be described in terms of anharmonic contributions V to the harmonic oscillator Hamiltonian H_0, which describes the uncoupled vibrational motion of the two "types" of molecules. Thus the well-known expression for the energies of the two coupled oscillators is obtained:

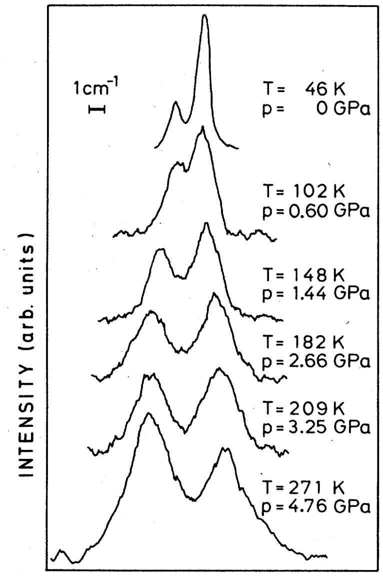

FIG. 7. Raman doublet in γ-O_2 at different temperatures and pressures. The zero-pressure spectrum is taken from Ref. 19.

$$E=(V_{aa}+V_{bb})/2\pm\tfrac{1}{2}[(V_{aa}-V_{bb})^2+4V_{ab}^2]^{1/2} \tag{1}$$

(for convenience $\Delta:=V_{bb}-V_{aa}$ and $[(V_{aa}-V_{bb})^2+4V_{ab}^2]^{1/2}:=S$ represents the total splitting of the doublet).

The levels are equally spaced around $(V_{aa}+V_{bb})/2$. Here V_{aa} and V_{bb} denote the eigenvalues of V between the unperturbed eigenfunctions of the molecules on site a and b, respectively. V_{ab} describes the coupling between molecule a and b. Consequently a mixing parameter c can be defined

$$c=(2V_{ab})/(V_{bb}-V_{aa})+[(V_{bb}-V_{aa})^2+4V_{ab}^2]^{1/2}\ . \tag{2}$$

This parameter determines the extent of mixing of the wave functions of the molecules a and b. Only if $c=0$ can each band of the spectrum be assigned to a special type of molecule. Consistently with increasing coupling V_{ab}, the splitting increases. In addition the intensities of both components are strongly influenced. Let N_a and N_b be the number of molecules on site a and b, I_a and I_b the respective intensities; the following ratio can be derived:

$$I_a/I_b=(N_a/N_b)\left[\frac{[1-c(N_b/N_a)^{1/2}]^2}{[1+c(N_a/N_b)^{1/2}]^2}\right]\ . \tag{3}$$

Combining Eqs. (1) and (2) one obtains an expression for the coupling constant V_{ab}:

$$V_{ab}=S(c/1+c^2)\ . \tag{4}$$

Here S represents the total splitting of the doublet and c the above-mentioned mixing parameter which are both measurable quantities and thus directly accessible from experiment, one from intensity considerations via Eq. (3), the other from frequency measurements.

As known from zero-pressure experiments,[19] $I_a/I_b=3{:}1$ and $\Delta(p=0)=1.3$ cm^{-1}. Consequently c and V_{ab} are equal to zero at $p=0$, which describes the uncoupled case. According to the phase diagram (Fig. 6) higher temperatures are needed to stabilize the γ phase at high pressures. Thus one could expect also temperature to affect the parameters c and S in the coupling constant V_{ab} in addition to pressure. However, if one extrapolates the frequency versus pressure plots for both vibrational components (see Fig. 4) to zero pressure, which was done at various fixed temperatures up to 240 K, one obtains a zero-pressure splitting in the range of 1–2 cm^{-1} in all cases. Therefore it is mainly volume change that drives the V-V resonant transfer interaction and one can restrict on a single parameter only in the following, namely, pressure.

According to Eq. (4) the pressure-dependent values for the coupling constant V_{ab} can be determined from the experimental values c and S compiled in Figs. 8(a) and 8(b), respectively. A plot, similar to Fig. 8(b) for the total splitting S only, was already presented by Yen *et al.*[20] Although their data points show a much greater statistical scattering than ours due to their lower spectral resolution, the overall effect is comparable with our data. Figure 8(c) presents values for the coupling constant V_{ab} as a function of pressure. These values increase almost linearly from 0 up to 1.6 cm^{-1} in the pressure range of 0—5 GPa.

Using these data of V_{ab}, one can derive pressure-dependent values for Δ, which represent the splitting of the vibrational doublet in the case of zero coupling. These data Δ are compiled in Fig. 8(b) together with the observed total splitting S. Comparison of both curves versus p demonstrates that only a minor part of the total splitting is caused by the resonant interaction between the oxygen molecules on the two different sites. Most of the apparent splitting results from the different pressure dependence of both components, regardless of any V-V interaction.

The strength of the resonant V-V transfer coupling can be estimated by relating the coupling constant V_{ab} to the splitting Δ (for strong coupling $V_{ab} \gg \Delta$). Thus the ratio $(V_{ab}/\Delta)^2$ increases from zero up to 0.15 in the range of 0—5 GPa. These small values imply very weak coupling with a tendency toward increasing strength with volume compression [for comparison the classical Fermi resonance in CO_2: $(V_{ab}/\Delta)^2=10$].

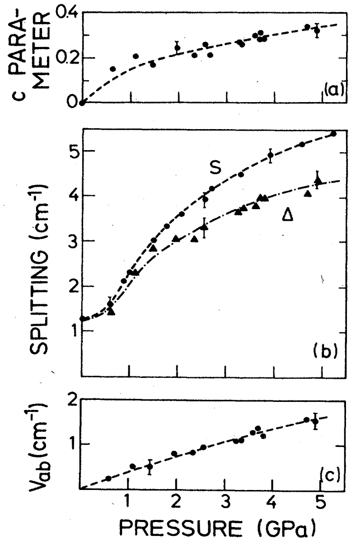

FIG. 8. (a) Mixing parameter c as a function of pressure [after Eq. (3) and data from Fig. 7]. (b) Pressure-dependent splitting of the vibrational doublet in γ-O_2. S, experimental values of the total splitting; Δ, splitting calculated for zero coupling. (c) Pressure-dependent interaction energy V_{ab} derived via Eq. (4).

D. Pressure dependence of the vibron and librons in α-O_2: Comparison of theory with experiment

High-pressure data can serve as a sensitive test for intramolecular and intermolecular potentials as long as pressure-dependent volume data or intermolecular distances of the material under compression are known. Recent calculations of the pressure-dependent vibron frequencies in β-O_2 at $T=0$ K (Ref. 25) and vibron as well as libron frequencies in α-O_2 at $T=0$ K (Ref. 26) have been reported, which can be tested using our experimental data. As for β-O_2 only experimental data are available in a reasonable pressure range for temperatures above 80 K, we restrict our discussion to α-O_2. Helmy *et al.*[26] have made two different approaches. In one they used the well-known English-Venables (EV) potential between nonbonded O atoms plus an electric quadrupole-quadrupole interaction term between pairs of molecules.[33] The internal potential was constructed using a Taylor-series expansion about the equilibrium interatomic distance with quadratic and cubic force constants taken from spectroscopic gas data.

In the second approach an r^{-6} attractive and $\exp(-ar)$ repulsive term instead of the Lennard-Jones potential used by English and Venables have been tested. In addition to an electric quadrupole-quadrupole term, similar to the one introduced by English and Venables,[33] a magnetic interaction was considered represented by a Heisenberg-exchange Hamiltonian. The exchange energy was taken from magnetic susceptibility measurements of Meier *et al.*[3]

The results of both models are pressure-dependent vibron and libron frequencies for α-O_2 at $T=0$ K shown in Fig. 9, which are displayed together with our experimental data at 10 K. For the vibron the simpler EV potential seems to fit better for the description of the pressure

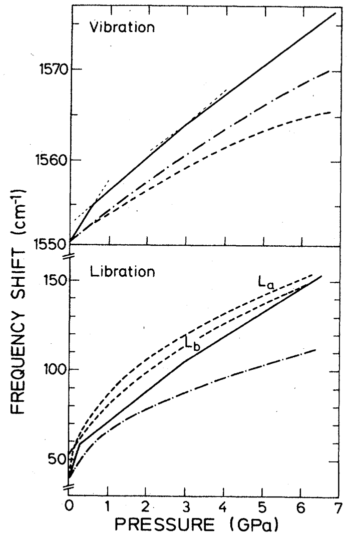

FIG. 9. Comparison of theory with experiment for the pressure dependence of the vibron and librons in α-O_2. Solid line, our experimental data at 10 K; dashed line, theory of Helmy *et al.* (Ref. 26); dashed-dotted line, English-Venables potential (Ref. 33).

behavior than the more sophisticated potential of Helmy *et al.*, which includes a magnetic interaction. In contrast to their potential the EV potential at least describes the general features of the pressure shift $(\partial\nu/\partial p)_T$ above 0.5 GPa quite well. Helmy *et al.* predict a much smaller slope $(\partial\nu/\partial p)_T$ than observed experimentally. Both theories do not, of course, consider any phase transition in that range, but assume the α structure to be stable up to 7 GPa, and can therefore not describe the changes in $(\partial\nu/\partial p)_T$, as observed in the experiment at the phase transitions.

Figure 9 (lower part) demonstrates rather good agreement between the theoretically predicted pressure dependence of the low-energy Raman-active mode (after Helmy *et al.*) with the one found experimentally, if one regards only the overall tendency. On the other hand, in contrast to the vibron the agreement of experimental and theoretical results based on the EV potential is now worse.

One last comment concerning the assignment of the two Raman modes of α-O_2 at about 43 and 79 cm^{-1} at zero pressure is noteworthy. According to group theory two modes of symmetries A_g and B_g are Raman active, the assignment seems straightforward. Several theoretical calculations,[8,26,34,35] whether magnetic interaction is incorporated or not, predicted at the Γ point two nearly degenerate librations (A_g,B_g) near 45 cm^{-1} with a separation of only 3–6 cm^{-1}.

Therefore theory cannot explain the high-energy mode in the Raman spectrum at 79 cm^{-1} as a single libron band. Thus the lower energy band is interpreted as the accidentally degenerate (A_g,B_g) mode, whereas the other band is explained as either a two-libron or a libron-magnon combination band. However, careful temperature-dependent Raman investigations at zero pressure[19] demonstrate that both lines exhibit the same temperature-dependent intensity behavior. Normally the temperature dependence of the intensity of a two-libron band is much stronger than that of a single-libron band, due to different Boltzmann factors. Thus the band at 43 cm^{-1} is most probably caused by the B_g libron, the other one by the A_g libron. Keeping this in mind new calculations seem to be necessary to solve this puzzle.

E. Anharmonic contributions to the intermolecular forces

Pressure has proven to be a good tool for the investigation of potentials in solids, especially of molecular crystals because of their high compressibility. This is caused by the weak intermolecular forces in contrast to the strong covalent intramolecular bonds. Thus pressure will influence both types of bonds in a different way. For example, applying pressures up to 7 GPa to α-O_2 will cause a contraction of lattice parameters of about 3%, whereas the bond length of the O_2 molecule is only compressed by 0.2% in the same pressure region.[26] This behavior is reflected in different pressure shifts $(\partial\nu/\partial p)_T$ of the vibration (order of 3–5 cm^{-1}/GPa) and of the librations (10–50 cm^{-1}/GPa) of solid oxygen.

The effect of temperature compared with pressure is more complicated, because in addition to volume expansion increasing temperature will also influence volume-independent parts of the anharmonic interaction, such as phonon-phonon interaction. Thus the experimental value of $(d\nu/dT)_p$ comprises both volume dependent (explicit contributions) and volume independent (implicit contributions) parts, namely, $(\partial\nu/\partial T)_V$. Both quantities are related in the following way:[36]

$$\left[\frac{d\nu}{dT}\right]_p = \left[\frac{\partial\nu}{\partial T}\right]_V - (\alpha/\beta_T)\left[\frac{\partial\nu}{\partial p}\right]_T \qquad (5)$$

(α, thermal-expansion coefficient; β_T, isothermal compressibility). In order to calculate the pure temperature-shift data for α and β_T are necessary in addition to $(d\nu/dT)_p$ and $(\partial\nu/\partial p)_T$ which can be derived from the pressure dependence of the vibron and libron frequencies at various temperatures.

Experimental data for the volume-expansion coefficient

TABLE I. Total temperature and pressure shifts of the vibrational and librational frequencies in the different phases of liquid and solid oxygen. High- and low-frequency components (HF and LF, respectively) of libration $(\alpha,\alpha',\bar{\alpha})$ and vibration (γ).

Phase	$\left[\frac{d\nu}{dT}\right]_p$ (cm^{-1}/K)	$\left[\frac{\partial\nu}{\partial p}\right]_T$ (cm^{-1}/GPa)
α		
vibron	−0.01	7.5 (6–27 K)
libron (LF)	−0.02	50 (6–27 K)
libron (HF)	−0.1	70 (6–27 K)
$\bar{\alpha}$		
vibron	−0.01	3.7 (6–98 K)
libron (LF)	−0.02	17.5 (6–98 K)
libron (HF)	−0.02	25.0 (6–98 K)
α'		
vibron	−0.01	3.0 (6–230 K)
libron (LF)	−0.02	13.3 (6–230 K)
libron (HF)	−0.02	16.6 (6–230 K)
β		
vibron	−0.02	5.0 (70 K)
vibron	−0.02	4.4 (80 K)
vibron	−0.02	3.0 (100–270 K)
libron	−0.2	20.0 (80–219 K)
γ		
(LF)		5.0
(HF)		7.5
(LF)		4.4
(HF)		6.0
(LF)		4.5
(HF)		5.2
ϵ		
vibron		2.7[a] (297 K)
libron (LF)	−0.09	10.0 (149 K)
libron (HF)	−0.09	11.3 (149 K)
vibron		3.3 (148 K)
vibron		5.0 (183 K)

[a] Room-temperature data from Ref. 30.

α are only available at zero pressure for α-, β-, γ-O_2.[8] In addition, available data for β_T are restricted to temperatures, where the three mentioned phases are stable at $p=0$. In contrast to this, most of our pressure- and temperature-shift data are obtained at higher temperatures and pressures. Under these restrictions one can calculate some values for the pure temperature shift $(\partial\nu/\partial T)_V$. As a result, one obtains values of the order of 10^{-2}—10^{-3} cm^{-1}/K for both the librons and the vibron without specific differences for the three phases α, β, and γ.

Finally data of the pressure and temperature shifts derived from the Raman spectra are listed in Table I. One can recognize that in most cases the total temperature shift $(d\nu/dT)_p$ is about ten times smaller for the vibron than for the librons. In all phases the pressure shifts for librons and the vibron are also significantly different, which, of course, reflects the different strength of intermolecular- and intramolecular bonds.

In the phases α, α', and $\bar{\alpha}$ the pressure shifts are independent of temperature for the vibron and the librons. In contrast to this the β phase shows a temperature-dependent pressure shift of the vibron with the tendency of decreasing $(\partial\nu/\partial p)_T$ with increasing temperature. This experimental fact clearly demonstrates that comparison of experimental data, especially obtained at higher temperatures, with theoretical ones (see Sec. III D) is sometimes problematic, because in most cases theoretical values are evaluated for $T=0$ K only.

F. Pressure-dependent mode-Grüneisen parameters

The different types of bonds in molecular solids are reflected in a different pressure response of external and internal modes, which was demonstrated in the preceding section for solid oxygen. A dimensionless parameter γ_i is often introduced (mode-Grüneisen parameter) which relates the pressure-induced frequency change of a special mode to the according volume change:

$$\gamma_i=\beta^{-1}\nu^{-1}\left[\frac{\partial\nu}{\partial p}\right]_T . \tag{6}$$

For external modes the Grüneisen parameter, denoted hereafter as γ_{ext}, is usually of the order of unity. For internal modes the corresponding parameter (γ_{int}) drops rapidly down to 10^{-2}—10^{-3} because of the small $1/\nu$ factor. On the other hand, Sherman[37] has shown that γ_{int} and γ_{ext} tend to approach the value of one in the limit of very high pressures.

For low pressures, where γ_{int} and γ_{ext} differ markedly, Zallen *et al.*[36] have introduced a so-called bond-scaling parameter γ', which is a measure of the bond anharmonicity. This bond-scaling parameter is then of the same magnitude as γ_{ext}.

As we have measured vibrational and librational frequencies in solid oxygen in a wide range of pressure, Sherman's model[37] of the pressure-dependent mode-Grüneisen parameters as well as the bond-scaling law can be tested, which can be written according to Zallen *et al.*:[36]

$$\gamma'=(k_{int}/k_{ext})(r/a)\gamma_{int} . \tag{7}$$

k_{int} and k_{ext} represent the respective force constants, r is for the equilibrium bond length of the molecule, and a is the lattice parameter. The ratio of the force constants can approximately be replaced by the squared ratio of the mode frequencies $(\omega_{int}/\omega_{ext})^2$.

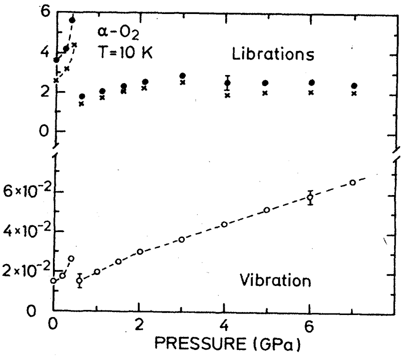

FIG. 10. Grüneisen parameters of the external and internal modes of α-O_2 as a function of pressure ($T=10$ K).

Due to the lack of sufficient data for β_T in other phases, only α-O_2 is considered here. The pressure-dependent isothermal compressibility was taken from volume-versus-pressure data of Helmy *et al.*[26] The resulting pressure-dependent values of γ_{int} and γ_{ext} are presented in Fig. 10. In the range of 0—7 GPa, γ_{int} increases from about 10^{-2} up to 7×10^{-2}. The γ_{ext} values, however, are in the range of 2—3 in the same pressure regime. A similar behavior can be observed for the case of β-O_2 (70 K). The Grüneisen parameters for the internal modes show a tendency to follow Sherman's model. The γ_{ext} values are more or less constant within the experimental uncertainty (see Fig. 10) with the slight tendency of decreasing values above 5 GPa.

Finally, bond-scaling parameters γ' can be evaluated according to Eq. (7). If data for lattice parameter a and bond length r are used from Ref. 26 and γ_{int} from Fig. 10 one obtains values in the range of 1.5—2 for α-O_2 as predicted from the bond-scaling law.

IV. CONCLUSION

It has been shown that Raman scattering is an excellent tool for the determination of the phase diagram of solid oxygen. The results of our measurements have enabled us to complete the phase diagram of oxygen in the temperature and pressure range from 6—300 K and 0—10 GPa, respectively. They also indicated the existence of a new high-pressure phase $\bar{\alpha}$ between the monoclinic α and orthorhombic α' phase.

Unfortunately our Raman study did not allow us to draw conclusions about the structure of the $\bar{\alpha}$ and ϵ phase, so that further x-ray studies are necessary to clarify these questions. Our study has also shown that the potentials used in the theoretical calculations must be modified to explain the pressure dependence of the frequencies of the vibration and librations at pressures above 1 GPa.

*Permanent address: FB Physik, Universität Kaiserslautern, Erwin-Schrödinger-Strasse, 6750 Kaiserslautern, Federal Republic of Germany.

[1] R. Muijlwijk, M. Durieux, and H. van Dijk, Physica **43**, 475 (1969).

[2] C. S. Barret, L. Meyer, and J. Wasserman, J. Chem. Phys. **47**, 592 (1967).

[3] R. J. Meyer and R. B. Helmholdt, Phys. Rev. B **29**, 1387 (1984).

[4] E. M. Hörl, Acta Crystallogr. **15**, 845 (1962).

[5] A. Alikhanov, J. Phys. (Paris) **25**, 449 (1964).

[6] T. H. Jordan, W. E. Streib, H. W. Smith, and W. N. Lipscomb, Acta Crystallogr. **17**, 777 (1964).

[7] Yu. B. Gaididei, V. M. Loktev, A. F. Prikhot'ko, and L. I. Shanskii, Fiz. Nizk. Temp. **1**, 1365 (1975) [Sov. J. Low Temp. Phys. **1**, 653 (1975)].

[8] I. N. Krupskii, A. I. Prokhvatilov, Yu. A. Freiman, and A. I. Erenburg, Fiz. Niak. Temp. **5**, 271 (1979) [Sov. J. Low Temp. Phys. **5**, 130 (1979)].

[9] H. d'Amour, W. B. Holzapfel, and M. Nicol, J. Phys. Chem. **85**, 130 (1981).

[10] T. Yagi, K. H. Hirsch, and W. B. Holzapfel, J. Phys. Chem. **87**, 2272 (1983).

[11] D. Schiferl, D. T. Cromer, L. A. Schwalbe, and R. L. Mills, Acta Crystallogr. Sect. B **39**, 153 (1983).

[12] J. E. Cahill and G. E. Leroi, J. Chem. Phys. **51**, 97 (1969).

[13] E. J. Wachtel and R. G. Wheeler, J. Appl. Phys. **42**, 1581 (1971).

[14] T. G. Blocker, M. A. Kinch, and F. G. West, Phys. Rev. Lett. **22**, 853 (1969).

[15] R. J. Meier, J. H. Colpa, and H. Sigg, J. Phys. C **17**, 4501 (1984).

[16] P. M. Mathai and E. J. Allin, Can. J. Phys. **48**, 1518 (1970).

[17] P. M. Mathai and E. J. Allin, Can. J. Phys. **49**, 1973 (1971).

[18] H. Kiefte, M. J. Clouter, N. H. Rich, and S. F. Ahmed, Chem. Phys. Lett. **70**, 425 (1980).

[19] K. D. Bier and H. J. Jodl, J. Chem. Phys. **81**, 1192 (1984).

[20] J. Yen and M. Nicol, J. Phys. Chem. **87**, 4616 (1983).

[21] H. D. Hochheimer, H. J. Jodl, W. Henkel, and F. Bolduan, Chem. Phys. Lett. **106**, 79 (1984).

[22] J. W. Stewart, J. Phys. Chem. Solids **12**, 122 (1959).

[23] R. J. Meier, C. J. Schinkel, and A. de Visser, J. Phys. C **15**, 1015 (1982).

[24] M. Nicol, K. R. Hirsch, and W. B. Holzapfel, Chem. Phys. Lett. **68**, 49 (1979).

[25] R. D. Etters and A. Helmy, Phys. Rev. B **27**, 6439 (1983).

[26] A. Helmy, K. Kobashi, and R. D. Etters, J. Chem. Phys. **80**, 2782 (1984).

[27] K. Hirsch and W. B. Holzapfel, Rev. Sci. Instrum. **52**, 52 (1981).

[28] R. A. Noack and W. B. Holzapfel, in *High Pressure Science and Technology,* edited by K. D. Timmerhaus and M. S. Barber (Plenum, New York, 1979), Vol. 1, p. 748.

[29] R. J. Meier, M. P. Van Albada, and Ad Lagendijk, Phys. Rev. Lett. **52**, 1045 (1984).

[30] K. Syassen and M. Nicol, in *Physics of Solids under High Pressure,* edited by J. S. Schilling and R. N. Shelton (North-Holland, Amsterdam, 1981), p. 33.

[31] M. Nicol and K. Syassen, Phys. Rev. B **28**, 1201 (1983).

[32] Y. Guissani, D. Levesque, J. J. Weis, and P. W. Otoxby, J. Chem. Phys. **77**, 2153 (1982).

[33] C. A. English and J. A. Venables, Proc. R. Soc. London, Ser. A **340**, 81 (1974); C. A. English and J. A. Venables, *ibid.* **340**, 57 (1974).

[34] K. Kobashi, M. L. Klein, and V. Chandrasekharan, J. Chem. Phys. **71**, 843 (1979).

[35] R. D. Etters, A. Helmy, and K. Kobashi, Phys. Rev. B **28**, 2166 (1983).

[36] R. Zallen and M. L. Slade, Phys. Rev. B **18**, 5775 (1978).

[37] W. F. Sherman, J. Phys. C **15**, 9 (1982).